

Polynomial transformation for MRI feature extraction

Hamid Soltanian-Zadeh,^{1,2} Mahmood Kharrat,^{1,3} Donald J. Peck²

¹Electrical and Computer Engineering Department, University of Tehran, Tehran 14399, Iran; ²Diagnostic Radiology Department, Henry Ford Health System, Detroit, MI 48202, USA; ³Information Technology Group, Iran Telecommunication Research Center, Tehran 14399, Iran

ABSTRACT

We present a non-linear (polynomial) transformation to minimize scattering of data points around normal tissue clusters in a normalized MRI feature space, in which normal tissues are clustered around pre-specified target positions. This transformation is motivated by non-linear relationship between MRI pixel intensities and intrinsic tissue parameters (e.g., T1, T2, PD). To determine scattering amount, we use ratio of summation of within-class distances for clusters to summation of their between-class distances. We find the transformation by minimizing the scattering amount. Next, we generate a 3D visualization of the MRI feature space and define regions of interest (ROI's) on clusters seen for normal and abnormal tissues. We use these ROI's to estimate signature vectors (cluster centres). Finally, we use the signature vectors for segmenting and characterizing tissues. We used simulation, phantom, and brain MRI to evaluate the polynomial transformation and compare it to the linear transformation. In all studies, we were able to identify clusters for normal and abnormal tissues and segment the images. Compared to the linear method, the non-linear approach yields enhanced clustering properties and better separation of normal and abnormal tissues. On the other hand, the linear transformation is more appropriate than the non-linear method for capturing partial volume information.

keywords: image segmentation, image analysis, tissue characterization, polynomial transformation, feature Space, Magnetic Resonance Imaging (MRI)

1. INTRODUCTION

A Common goal in a wide variety of disciplines, including speech science, psychology, economics, and medical science, is to correlate continuous valued measurements of “objects” with perceptual or interpretable variables which also describe those objects. In medical image analysis, the ultimate goal is to extract important clinical information that would improve diagnosis and treatment of disease.

One of the most useful medical imaging modalities is magnetic resonance imaging (MRI). The image gray levels in MRI depend on several tissue parameters including: spin density (SD), spin-lattice (T1) and spin-spin (T2) relaxation times, flow velocity (v), and chemical shift (δ). The first three parameters are most important in clinical imaging.^{1,2,8} A sequence of MRI images of the same anatomical site (an MRI scene sequence) contains information pertaining to the tissue parameters. These images prepare a multi-dimensional feature space.

An MRI scene sequence shows spatial location of different tissues, with different contrast in each image. It can therefore be considered as spatial domain representation of tissues. In a spatial domain representation, pixels corresponding to specific tissues are locally connected but may be distributed over different sections of the image. A feature space representation of the tissues can be generated from an MRI scene sequence. In a feature space representation, pixels corresponding to a specific tissue are connected as clusters, even though their spatial locations in the image domain may be far apart. For an MRI scene sequence consisting of n images, a feature space representation is generated by defining an n -dimensional (n -D) pixel vector for each pixel in the image (spatial) domain, using pixel gray levels of the same location from different images in the sequence as elements of this vector.

Image analysis can be accomplished using an appropriate feature space method. Feature space methods can be useful for all three steps of image analysis: 1) identification of objects; 2) segmentation of

objects; and 3) quantitative measurements on objects, to obtain information that can be used in decision making (diagnosis, treatment planning, and evaluation of treatment).³

In a computerized image analysis system, the input image is first preprocessed. Preprocessing may involve restoration, enhancement, or just proper representation of the data. Then certain features are extracted for segmentation of the image into its components. The segmented image is fed into a classifier or an image understanding system. Image classification assigns regions segmented to one of several objects. Image understanding subsystem determines the relationships between different objects in the scene in order to provide its description.⁵

In recent years, research work has been done in the field of MRI segmentation in which multi-parametric (multi-spectral) nature of MRI data is used.^{3,4,9} Feature extraction is a crucial step for MRI segmentation. Rather than using all the information in the images at once, feature extraction and selection breaks down the problem of segmentation to the grouping of feature vectors. Features can be pixel intensities themselves, feature calculated from the pixel intensities, or edge and texture features.

Often feature extraction is performed for visualization. Also, the proposed segmentation method in this paper is based on visualization of the generated feature space, i.e., visualization of the multi-dimensional histogram of the data, which is called a cluster plot. This constrains the dimensionality of the feature space. As the dimensionality of the feature space increases, its visualization becomes more difficult. One- and two-Dimensional (1-D and 2-D) feature spaces can easily be visualized using a conventional histogram, and an image whose pixel intensity is proportional to the number of data points in a certain range, i.e., a 2-D cluster plot. We may generate a three-Dimensional (3-D) cluster plot, by drawing three axes of an orthogonal coordinate system in an image, for 3-D perception, and making image pixel gray levels proportional to the number of data points in certain ranges.

There are several approaches for generating MRI feature space which can be partitioned into three categories:³ 1) tissue-parameter-weighted images; 2) explicit calculation of tissue parameters; and 3) linear and non-linear transformations. Due to the non-linearity of transformation from tissue parameter space to pixel intensity space, as illustrated in MRI signal equations (Bloch equations),^{1,2,9} optimal linear decision functions in tissue parameter space translate to non-linear decision functions in the intensity space. Thus, unless these non-linear decision functions are used, the decision is not optimal. There are some restrictions in using these categories, but category 3) can be applied to almost any MRI scene sequence. It can improve the clustering properties of data for the feature space representation while reducing its dimensionality.

We have devoted our effort towards the derivation of an optimal polynomial transformation to prepare MRI data for feature space analysis. It should be noted that an important distinction for feature extraction methods is whether they need class information or not. The method proposed in this paper needs some class information (signature vector for normal tissues) and is compatible to MRI needs.

The features extracted from the image, define clusters in the feature space. There is a correspondence between these clusters and the tissue types in the image. We explore this correspondence to segment the scene using the information present in the cluster plot. Visualization of the feature space (cluster plot) is therefore critical to the proposed method.

The next step in our approach is prototype identification. The signature vectors for these prototypes are used in scene segmentation by the nearest prototype classifier. A sensible method for prototype identification is looking at multi-dimensional histogram (cluster plot) of the data. We restrict our attention to feature space with dimensions smaller than four, so that they can be visualized and used by radiologists for diagnosis. We therefore want to reduce the dimensionality of the data to three, while improving its clustering properties. Further, for easy distinction between normal and abnormal issues, we would like to cluster each of the normal tissues around a pre-specified location. This should result in clustering abnormal tissues around different locations.

In the cluster plot, a 3-D vector represents each pixel. We generate a 2-D view (perspective) of the cluster plot for these 3-D pixel vectors. From the cluster plot, we are able to define several cluster centers corresponding to different tissue types, and segment the scene into these tissues using a Euclidean distance classifier (the nearest prototype classifier). Tissue localization and measurement can then be performed using the segmented scenes for several slices through the desired volume.

2. PREVIOUS METHODS

As mentioned above, there are different methods for generating MRI feature space. For example, principle component analysis (PCA) is a linear transformation, which has been employed in digital image processing as a technique for image coding, compression, enhancement, and feature extraction.⁶ For MRI feature representation, PCA generates linear combinations of the acquired images, which maximize the image variance. The weighting vectors for these linear combinations are the normalized eigenvectors of the sample covariance matrix. The number of principle component images equals the number of acquired images, but the variance (equivalently global SNR) of the principal component images sharply decreases from the first image to the last. The first three principal component images contain most of the information and hence may be used to define a 3-D feature space representation of the tissues.

Another 3-D feature space method generates angle images⁴ by calculating a set of parameters for each pixel vector in an orthogonal subspace defined by the constant vector ($C_v=[1,1,\dots,1]^T$) and the signature vector for normal tissues (S_i , $i= 1,\dots,M$, where M is the number of normal tissue types) that are encountered in a study, e.g., white matter, gray matter, and CSF for the brain. As shown in reference,⁴ among all of the possibilities for a 3-D feature space, the feature space generated by: 1) the Euclidean norm of each pixel vector; 2) the angle between each vector and the constant vector; 3) the angle between each pixel vector and the orthogonal complement of white matter to the constant vector, best separates normal and abnormal tissues in a brain study.

One of the most successful methods for human brain MRI feature extraction is optimal linear transformation of Soltanian-Zadeh, et al.³ In this method, the MRI data is prepared for feature space analysis using linear minimum mean square error transformation of categorical data to target positions. The transformation maps all pixel vectors from each tissue in the original feature space to tightly clustered regions in the transformed subspace (3-D subspace). Optimality is achieved in the sense that the tightest possible clusters are obtained under the constraint that normal tissues cluster at target positions. Qualitative and quantitative experimental results showed that, among existing methods, the optimal linear transformation has the best performance for MRI feature space analysis.³ In this paper, we compare the proposed optimal polynomial transformation to the optimal linear transformation.

3. PROPOSED METHOD

Efficacy of a feature extraction method depends on the nature of the data and the type of classifier used.^{5,7} As mentioned in the Introduction, there is a nonlinear relationship between pixel intensity space and tissue parameter space. This motivated us to develop a non-linear polynomial transformation.

Let \underline{V} be an N -dimensional real-valued vector space. Similarly, let \underline{C} be a P -dimensional real-valued vector space. Then data points in \underline{V} and \underline{C} are vectors in \mathbb{R}^N and \mathbb{R}^P , respectively. Further, assume that a collection of data can be classified or categorized in terms of M predefined groups, with data points within a group more “similar” to other data points in that group than to the data in other groups. Let each data category have a target position in \underline{C} about which transformed data are expected to cluster well. Denote the number of data points in each category as $NS(j)$, $j=1, \dots, M$. A non-linear transformation $F(\cdot)$ is desired which maps points in \underline{V} to points in \underline{C} as follows.

$$C = F(V) \quad (1)$$

Suppose that the i th element of C is:

$$C_i = \sum_{j=1}^N T_{ij} v_j + O_i + \sum_{j=1}^N \sum_{k=j}^N W_{ijk} v_j v_k, \quad i=1,\dots,P \quad (2)$$

The terms T 's, O 's, and W 's are to be found such that the mean-square error averaged over the training data set, between specified target positions in \underline{C} and projections from the measurement space, is minimized. That is, T , O and W will transform data from \underline{V} to \underline{C} such that the data in each category will cluster around pre-specified target position in \underline{C} as tight as possible in the mean-square error sense. This error can be formulated as follows. Choose M vectors in \underline{C} , each of which represents a distinct target position in the transformed space. From these vectors, form the $P \times M$ matrix C , each of whose columns is one of the target

vectors chosen. Then C_{ij} is the i th component of the j th target vector. Similarly, form a triple-indexed array v , such that v_{ijk} is the i th component of the k th data point in category j in the original space. With these notations, the mean-square “projection” error for a particular data point in the j th category is given by:

$$D_{jk} = \sum_{i=1}^P (c_{ij} - [\sum_{l=1}^N T_{il} v_{ljk} + O_i + \sum_{r=1}^N \sum_{s=r}^N W_{irs} v_{rjk} v_{sjk}])^2 \quad (3)$$

Summing over all M data categories and the number of data points in each category $NS(j)$, the total mean-square projection error is:

$$D = \sum_{j=1}^M \sum_{k=1}^{NS(j)} \sum_{i=1}^P (c_{ij} - [\sum_{l=1}^N T_{il} v_{ljk} + O_i + \sum_{r=1}^N \sum_{s=r}^N W_{irs} v_{rjk} v_{sjk}])^2 \quad (4)$$

We thus need to determine all elements of $T(T_{mn}, 1 \leq m \leq P, 1 \leq n \leq N)$, $O(O_m, 1 \leq m \leq P)$ and $W(W_{myt}, 1 \leq m \leq P, 1 \leq y \leq N, y \leq t \leq N)$ such that D is minimized. Taking the partial derivatives of D with respect to each T_{mn} , each O_m , and each W_{myt} and setting these derivatives equal to zero can accomplish this. With this approach, the followings of equations are obtained.

$$\frac{\partial D}{\partial T_{mn}} = \sum_{j=1}^M \sum_{k=1}^{NS(j)} -2(c_{mj} - [\sum_{l=1}^N T_{ml} v_{ljk} + O_m + \sum_{r=1}^N \sum_{s=r}^N W_{mrs} v_{rjk} v_{sjk}]) v_{njt} \quad \begin{matrix} 1 \leq m \leq P \\ 1 \leq n \leq N \end{matrix} \quad (5)$$

$$\frac{\partial D}{\partial O_m} = \sum_{j=1}^M \sum_{k=1}^{NS(j)} -2(c_{mj} - [\sum_{l=1}^N T_{ml} v_{ljk} + O_m + \sum_{r=1}^N \sum_{s=r}^N W_{mrs} v_{rjk} v_{sjk}]) \quad 1 \leq m \leq P \quad (6)$$

$$\frac{\partial D}{\partial W_{myt}} = \sum_{j=1}^M \sum_{k=1}^{NS(j)} -2(c_{mj} - [\sum_{l=1}^N T_{ml} v_{ljk} + O_m + \sum_{r=1}^N \sum_{s=r}^N W_{mrs} v_{rjk} v_{sjk}]) v_{yjk} v_{tik} \quad \begin{matrix} 1 \leq m \leq P, \\ 1 \leq y \leq N, \\ y \leq t \leq N \end{matrix} \quad (7)$$

Setting the derivatives equal to zero results in the following $P[N + 1 + (N + 1)/(N / 2)]$ equations needed to find elements of T , O , and W .

$$\sum_{j=1}^M \sum_{k=1}^{NS(j)} c_{mj} v_{njt} = \sum_{j=1}^M \sum_{k=1}^{NS(j)} (\sum_{l=1}^N T_{ml} v_{ljk} + O_m + \sum_{r=1}^N \sum_{s=r}^N W_{mrs} v_{rjk} v_{sjk}) v_{njt} \quad (8)$$

$$\sum_{j=1}^M \sum_{k=1}^{NS(j)} c_{mj} = \sum_{j=1}^M \sum_{k=1}^{NS(j)} (\sum_{l=1}^N T_{ml} v_{ljk} + O_m + \sum_{r=1}^N \sum_{s=r}^N W_{mrs} v_{rjk} v_{sjk}) \quad (9)$$

$$\sum_{j=1}^M \sum_{k=1}^{NS(j)} c_{mj} v_{yjk} v_{tik} = \sum_{j=1}^M \sum_{k=1}^{NS(j)} (\sum_{l=1}^N T_{ml} v_{ljk} + O_m + \sum_{r=1}^N \sum_{s=r}^N W_{mrs} v_{rjk} v_{sjk}) v_{yjk} v_{tik} \quad (10)$$

Equations (8)-(10) can be combined and rewritten as sets of matrix equations:

$$AX = b \quad (11)$$

where A is a square matrix, X is a column vector of unknowns, and b is a column vector. The m th matrix equation is used to solve for the m th transformation coefficients. The elements of A are:

$$A_{bc} = \sum_{j=1}^M \sum_{k=1}^{NS(j)} v_{cjk} v_{bjk} \quad (1 \leq b \leq N), (1 \leq c \leq N) \quad (12)$$

$$A_{bc} = \sum_{j=1}^M \sum_{k=1}^{NS(j)} v_{bjk} \quad (1 \leq b \leq N), (c = N + 1) \quad (13)$$

$$A_{bc} = \sum_{j=1}^M \sum_{k=1}^{NS(j)} v_{yjk} v_{tjk} v_{bjk} \quad (c, y, t) = \{(N+1, 1, 1), (N+2, 1, 1), \dots, (\sum_{l=1}^N l, N, N)\} \\ (1 \leq b \leq N) \quad (14)$$

$$A_{bc} = \sum_{j=1}^M \sum_{k=1}^{NS(j)} v_{cjk} \quad (b = N + 1), (1 \leq c \leq N) \quad (15)$$

$$A_{bc} = \sum_{j=1}^M \sum_{k=1}^{NS(j)} 1 \quad (b = N + 1), (c = N + 1) \quad (16)$$

$$A_{bc} = \sum_{j=1}^M \sum_{k=1}^{NS(j)} v_{yjk} v_{tjk} \quad (c, y, t) = \{(N+1, 1, 1), (N+2, 1, 1), \dots, (\sum_{l=1}^N l, N, N)\} \\ (b = N + 1) \quad (17)$$

$$A_{bc} = \sum_{j=1}^M \sum_{k=1}^{NS(j)} v_{yjk} v_{tjk} v_{cjk} \quad (b, y, t) = \{(N+1, 1, 1), (N+2, 1, 1), \dots, (\sum_{l=1}^N l, N, N)\} \\ (1 \leq c \leq N) \quad (18)$$

$$A_{bc} = \sum_{j=1}^M \sum_{k=1}^{NS(j)} v_{yjk} v_{tjk} \quad (b, y, t) = \{(N+1, 1, 1), (N+2, 1, 1), \dots, (\sum_{l=1}^N l, N, N)\} \\ (c = N + 1) \quad (19)$$

$$A_{bc} = \sum_{j=1}^M \sum_{k=1}^{NS(j)} v_{yjk} v_{tjk} v_{xjk} v_{wjk} \quad (b, y, t) = \{(N+1, 1, 1), (N+2, 1, 1), \dots, (\sum_{l=1}^N l, N, N)\} \\ (c, x, w) = \{(N+1, 1, 1), (N+2, 1, 1), \dots, (\sum_{l=1}^N l, N, N)\} \quad (20)$$

The m th unknown vector in Equation (11) is:

$$X^T = [T_{m1}, T_{m2}, \dots, T_{mN}, O_m, W_{m11}, W_{m12}, \dots, W_{mNN}] \quad (21)$$

Finally, the elements of b are given by:

$$b^T = \left[\sum_{j=1}^M \sum_{k=1}^{NS(j)} c_{mj} v_{1jk}, \dots, \sum_{j=1}^M \sum_{k=1}^{NS(j)} c_{mj} v_{Njk}, \sum_{j=1}^M \sum_{k=1}^{NS(j)} c_{mj}, \right. \\ \left. \sum_{j=1}^M \sum_{k=1}^{NS(j)} c_{mj} v_{1jk} v_{1jk}, \dots, \sum_{j=1}^M \sum_{k=1}^{NS(j)} c_{mj} v_{Njk} v_{Njk} \right] \quad (22)$$

By solving m matrix equations, the coefficients of T , O , and W are determined. A unique solution is guaranteed if the matrix A is non-singular and thus invertible.

4. EXPERIMENTAL RESULTS

All of the experimental results presented in this paper have been obtained using a SUN Sparcstation 10, and the visualization of the 3-D cluster plots and segmentation process have been done using Eigentool software, developed in Image Analysis Laboratory, Department of Radiology, Henry Ford Health System, Detroit, MI 48202, USA.

Before applying the transformation, we apply a multi-dimensional non-linear edge-preserving filter to suppress the MRI noise.³ Then, we define an n -D ($n > 3$) vector for each pixel, by using the corresponding image gray levels as elements of this vector. We refer to such a vector as a pixel vector. Similarly, we define n -D signature vectors for three of the normal tissues, by using the mean values of the image gray levels in sample ROI's corresponding to these tissues. A sample ROI should be a pure region from the tissue type (the bigger the ROI the better). Using this information, we find the optimal polynomial transformation and apply it to the MRI scene sequence to generate three composite images. For brain studies, the composite images are generated for white matter, gray matter, and CSF. Using these composite images, each pixel is now represented by a 3-D pixel vector. For these vectors, a perspective view of the cluster plot is generated. An image gray level in this cluster plot represents the number of pixel vectors whose components fell in a certain range; this range depends on the location of the pixel on the cluster map. For brain studies, the normal tissues are clustered around the tips of the unit vectors in the 3-D cluster plot. The abnormal tissues are clustered around different locations. From the cluster plot, we define several cluster centers (ROI's) corresponding to different tissue types. These are called ROI's since they are drawn on a perspective view of the 3-D cluster plot. New signature vectors are defined by averaging image gray levels, from the original or transformed images, which correspond to the ROI's drawn on the cluster plot. Using these signature vectors and the nearest prototype classifier, the scene is segmented.

We have compared the proposed feature space method to the optimal linear transformation method. We have found three performance measures for the two methods: 1) the distances between centers of the normal tissue clusters and centers of the abnormal tissue clusters; 2) the dispersion of samples within the training ROI's in the transformed space; and 3) the ability to distinguish between different clusters in the cluster plot by visual inspection. Experimental results, presented below, show that the first performance measure is larger and the second is smaller for the proposed method, compared to the previous method.

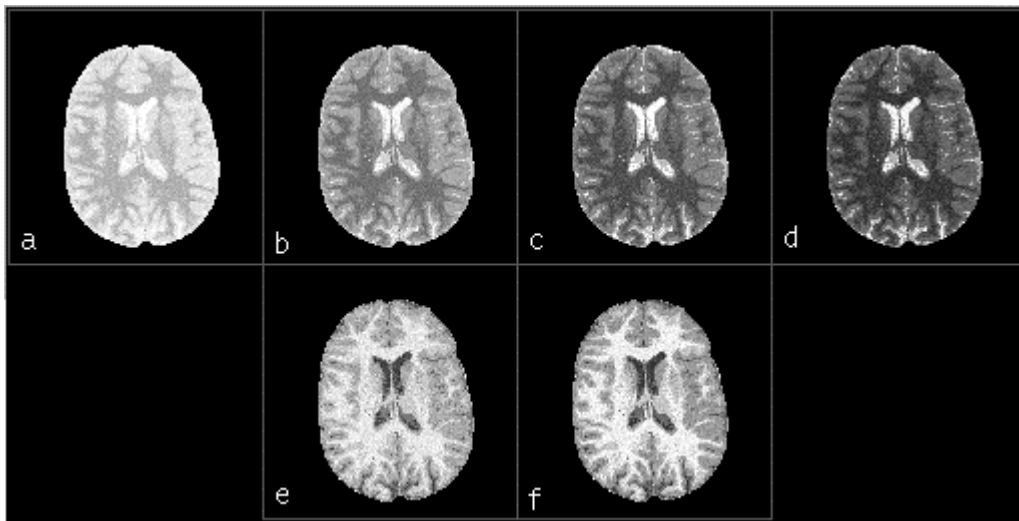


Fig. 1. Original images of a brain simulation.

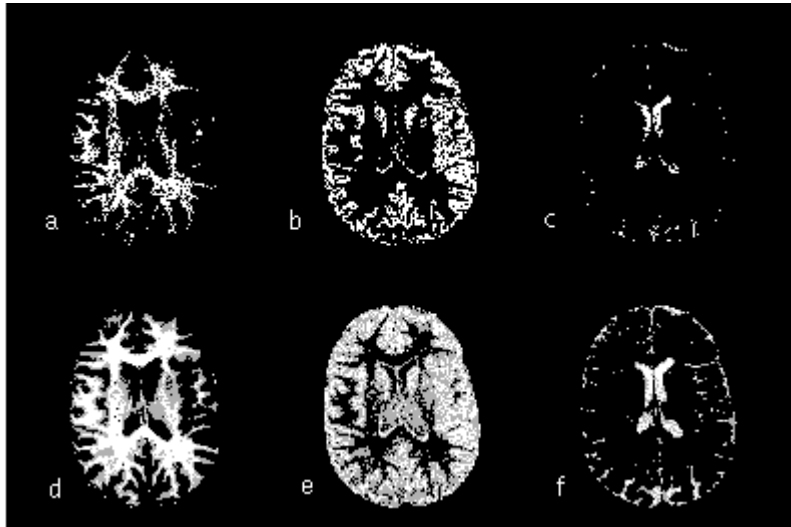


Fig. 2. Composite images obtained from images in Fig. 1 using the linear transformation (a to c) and the polynomial transformation (d to f).

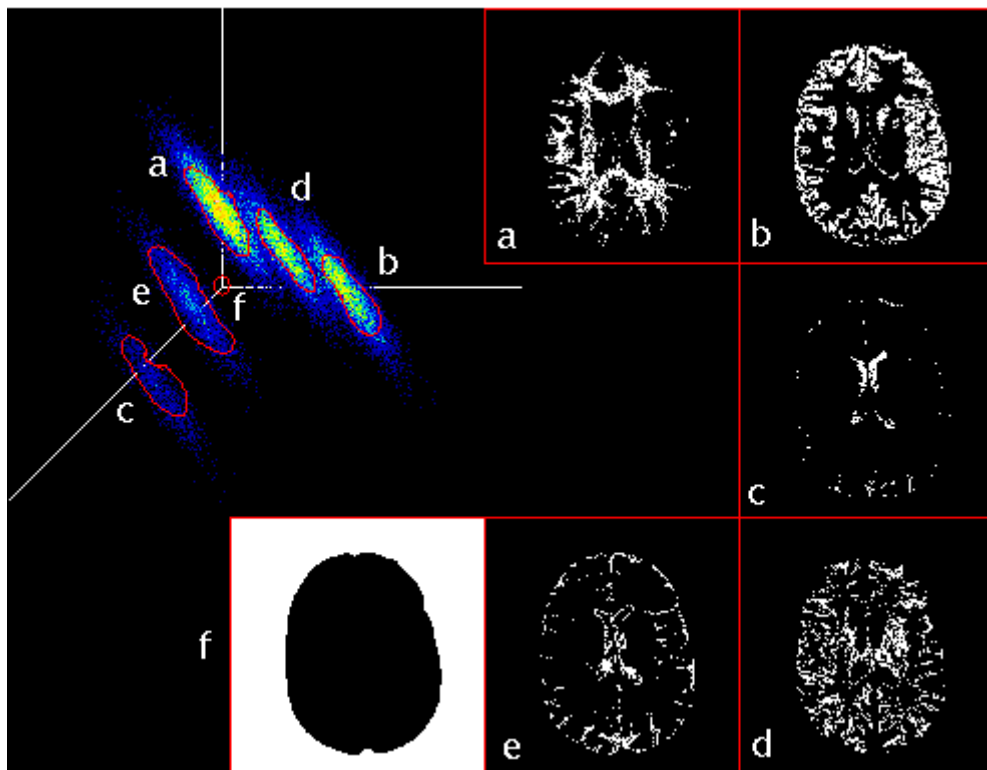


Fig. 3. Cluster plot and segmented images for the feature space defined by the images in the first row of Fig. 2 (optimal linear transformation).

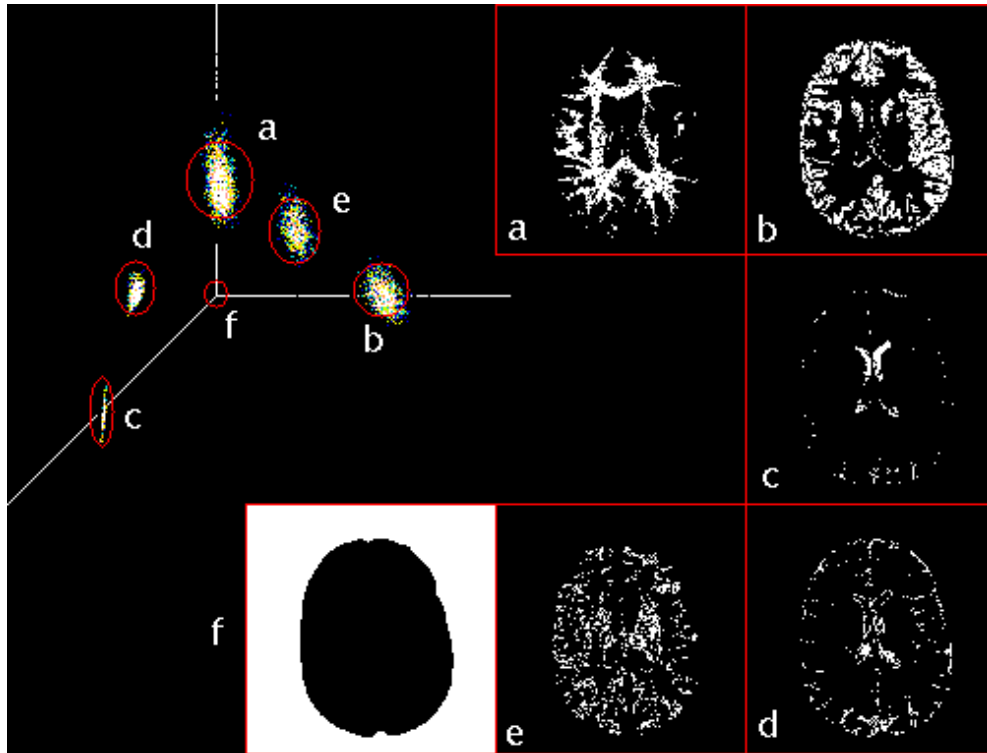


Fig. 4. Cluster plot and segmented images for the feature space defined by the images in the second row of Fig. 2 (optimal polynomial transformation). Note compactness of the clusters compared to those in Fig. 3.

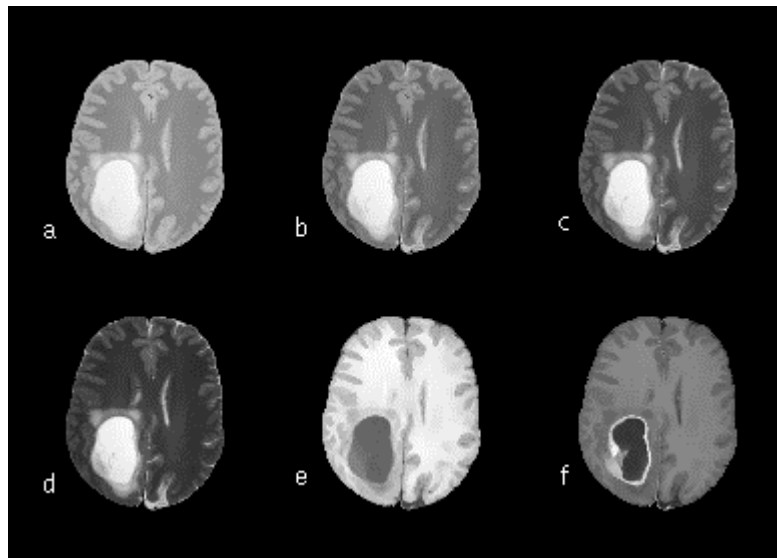


Fig. 5. Original images of a patient brain.

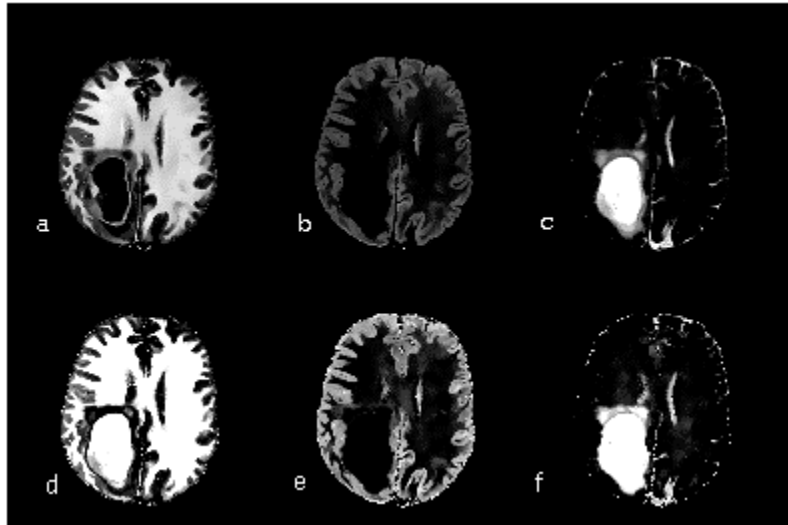


Fig. 6. Composite images obtained from images in Fig. 5, using the optimal linear transformation (a to c) and the optimal polynomial transformation (d to f).

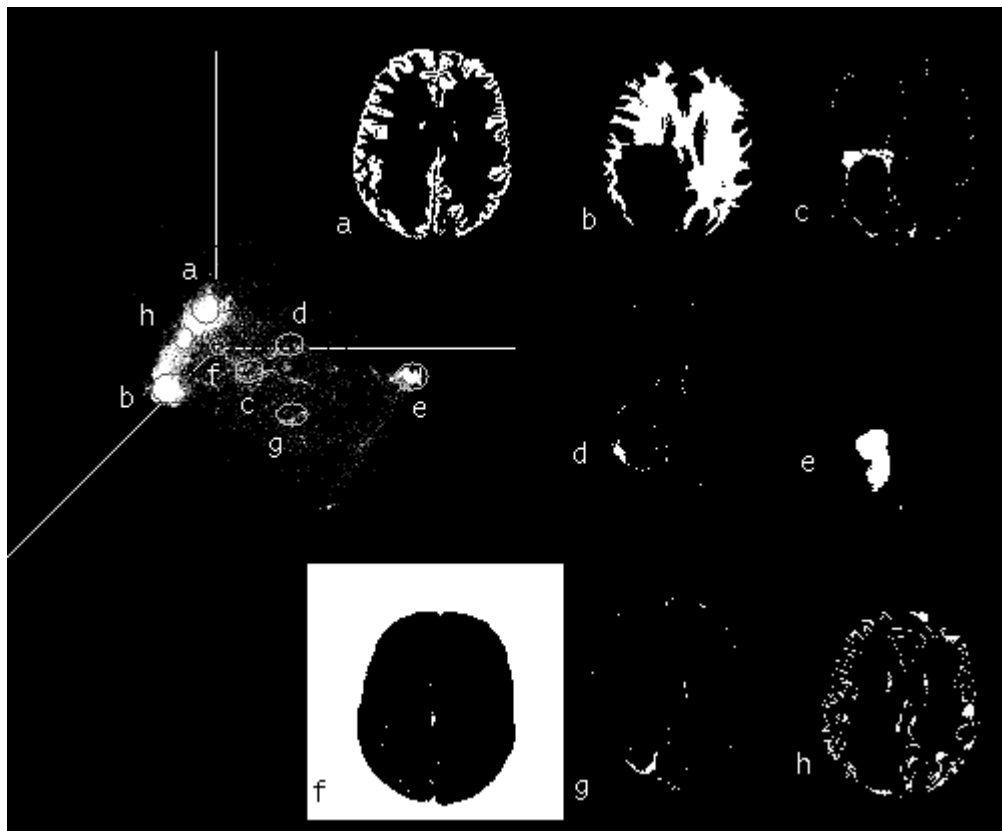


Fig. 7. Cluster plot and segmented images for the feature space defined by images in the first row of Fig. 6 (optimal linear transformation).

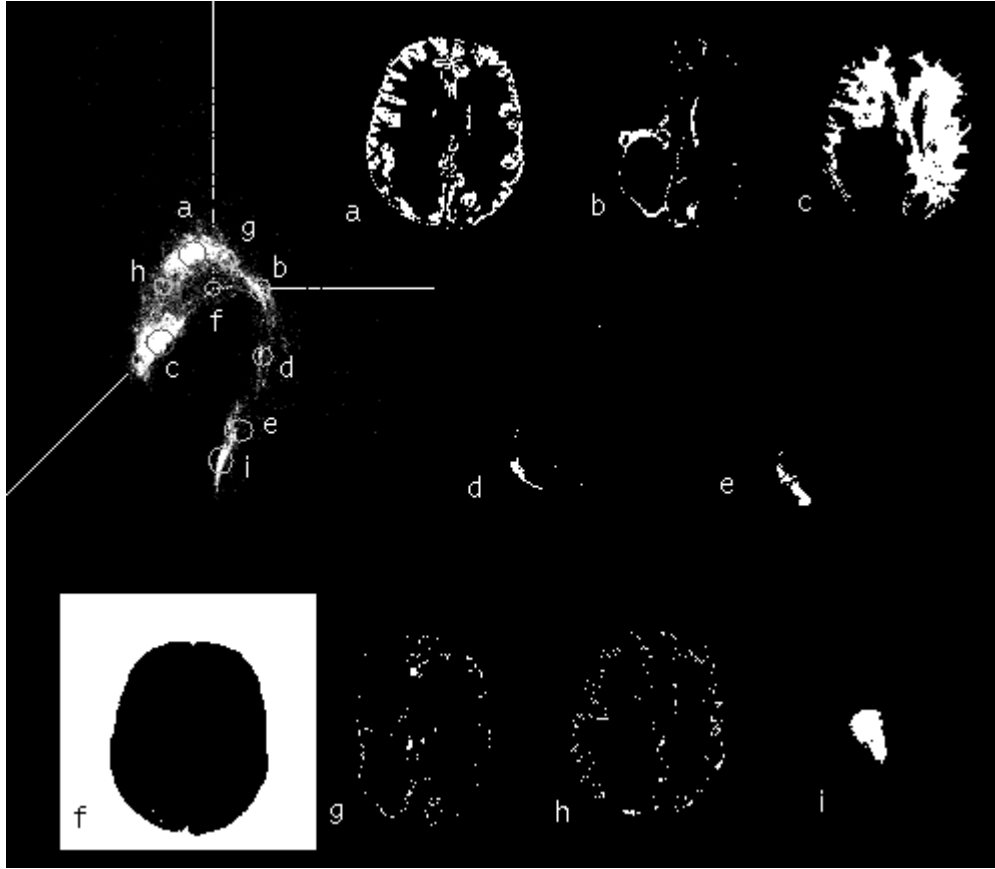


Fig. 8. Cluster plot for the feature space defined by the images in second row of Fig. 6 (optimal polynomial transformation). Note compactness of the clusters compared to those in Fig. 7.

Fig. 1 shows an MRI scene sequence of a brain simulation. The simulation is generated using the signature vectors and structures of the human brain tissues. A white Gaussian noise field with a standard deviation similar to that of acquired images is also used in generating the simulated images. The simulated scene contains white matter, gray matter, and CSF. Fig. 5 shows a real MRI study of a patient's brain with a lesion (which has three different parts).

Transformed images of the simulation study are shown in Fig. 2. The cluster plots generated using images in each of the two rows of Fig. 2 are shown in Figs. 3 and 4, respectively. In these Figures, the segmented tissues using ROI's are also shown. Note that the clusters in Fig. 4 are more compact and further separated compared to those in Fig. 3. The transformed images and cluster plots of the patient study are shown in Figs. 7 and 8, respectively. Note similar improvement for the patient study.

Table 1. Dispersion of the samples in the training ROI's for simulated brain images in the transformed space. This table shows 49.52% improvement in total mean square projection error by the optimal polynomial transformation, compared to the optimal linear transformation.

Tissue Model	CSF	Gray Matter	White Matter
Optimal Linear	1.1396	0.7219	0.651
Optimal Polynomial	0.5401	0.3476	0.3811

Table 2. Dispersion of the samples in the training ROI's for patient brain images in the transformed space. This table shows 33.40% improvement in the total mean square projection error by the optimal polynomial transformation, compared to the optimal linear transformation.

Tissue	CSF	Gray Matter	White Matter	lesion
Model				
Optimal Linear	1.5868	0.3566	0.1615	0.0892
Optimal Polynomial	0.9763	0.2743	0.1512	0.1618

Table 3. Distances between centers of the normal tissue clusters and centers of the abnormal tissue clusters for the patient study.

Tissue	CSF	Gray Matter	White Matter
Model			
Optimal Linear	2.5343	3.7940	3.8517
Optimal Polynomial	3.1934	4.3730	3.1500

The dispersion of sample ROI's in the target space, for the simulated and real MR images are shown in Tables 1 and 2, respectively. They show that the optimal polynomial method generates feature spaces with more compact clusters compared to the optimal linear method. Considering other studies of simulated, phantom, and human MRI (not shown in this paper), the polynomial method generated an average of 39.78% improvement for the mean square projection error.

Table 3 shows distances between centers of normal tissue clusters and centers of abnormal clusters for the patient study. This table illustrates that the distances between the normal and abnormal tissue clusters are greater in the clusters generated by the optimal polynomial transform compared to those generated by the optimal linear method.

5. CONCLUSION

Experimental results demonstrated efficacy of the polynomial transformation for MRI feature space analysis. Compared to the linear method, the proposed polynomial method yields improved clustering properties and separation of normal and abnormal tissue clusters using MRI. However, the linear transformation is more appropriate than the polynomial method for capturing the partial volume information from the cluster plots.

REFERENCES

1. A.D.Elater, *Questions and Answers in Magnetic Resonance Imaging*, Mosby Year Book, New York, NY, 1994.
2. H. Soltanian-Zadeh, *Ph.D Dissertation, Chapter 2*, University of Michigan, Ann Arbor, 1992.
3. H. Soltanian-Zadeh, J. P. Windham, D. J. Peck, "Optimal Linear Feature Extracion For MRI Images," *IEEE Trans. Medical Imaging*, Vol. 15, No. 6, pp. 749-767, Dec. 1996.
4. J. P. Windham, H. Soltanian-Zadeh, D. J. Peck, "Tissue Characterization by a Vector Subspace Method," *Med. Phys.*, Vol. 18, No. 3, pp. 619, 1991.
5. K. Fukunaga, *Introduction to Statistical Pattern Recognition*, Second edition, Academic Press, New York, NY, 1990.
6. R. Gonzalez, R. Woods, *Digital Image Processing*, Addison-Wesley, Boston, MA, 1992.
7. S. A. Zoharian, A. J. Jarghaghi, "Minimum Mean Square Error Transformation of Categorical Data to Target Positions," *IEEE Trans. Signal Processing*, Vol. 40, No. 1, pp. 13-23, 1992.
8. S. C. Bushong, *Magnetic Resonance Imaging Physical and Biological Principles*, Mosby Year Book, New York, NY, 1996.
9. S. E. Umbaugh, Y. Wei, M. Zuke, "Feature Extraction in Image Analysis," *IEEE Eng. in Med. and Bio.* pp. 62-73, Jul /Aug 1997.